Journal of Sound and Vibration (1994) **177**(1), 31–41

DETERMINATION OF RIGID BODY CHARACTERISTICS FROM TIME DOMAIN MODAL TEST DATA

S. M. PANDIT and Z.-Q. HU

Department of Mechanical Engineering and Engineering Mechanics, Michigan Technological University, Houghton, Michigan 49931, *U.S.A.*

(*Received* 20 *May* 1991, *and in final form* 20 *May* 1993)

A new method is presented to identify the characteristics of a rigid body and its supports, such as the center of gravity, the moment of inertia, and the stiffness and damping matrices, based on the measured time domain vibration data. Transformation matrices are formed using only the geometric co-ordinates relative to an arbitrarily selected origin to relate the pure translational measurement to both translation and rotation of the rigid body system. The rigid body modes and mode shapes, carefully selected from the accurately determined modes and mode shapes (rigid body and structural), are used, together with the special matrix structure, such as symmetry. The test result shows that the center of gravity and the moment of inertia are determined with good accuracy. The simple test procedure makes it an easily implementable method in practice.

1. INTRODUCTION

A rigid body and its supports form a dynamic system which is commonly used in many mechanical structures. The function of the supports is to hold the rigid body and to isolate the noise and vibration from other structures. Characteristics such as center of gravity and moment of inertia are the indispensable parameters for understanding rigid body motion. Together with system stiffness and damping matrices, they form the basis for analysis [1, 2], simulation [3], decoupling and isolation [4] and optimization [5–7] of many mechanical systems, particularly engine mount systems. For very simple structures, or structures composed of simple components, the center of gravity and the moment of inertia can be calculated from their geometry. However, for complex structures such calculation is very difficult. The pendulum test takes special skill and is prone to large experimental error; it is also time-consuming and dangerous. The method proposed by N. Okubo and T. Furukawa [8] determines these parameters by minimizing the difference between the values of the frequency response function (FRF) in the low frequency range and those calculated by these rigid body mode parameters. The direct system identification method (DSIM) [9] determines the six-degree-of-freedom (6-DOF) rigid body characteristics of engine mount system by minimizing the mean squared error between the measured FRF and the FRF calculated from the 6-DOF rigid body equations of motion. A better algorithm is proposed in references [10, 11] based upon the maximum likelihood estimation to improve the accuracy. Both methods rely on a specific low frequency range containing only rigid body modes. These methods are not applicable if this rigid body mode range does not exist and the elastic modes and the rigid body modes are mixed in the same range. The DSIM method uses a 6-DOF model to match the measured FRF; this implies that all six rigid body modes must be excited; otherwise, even a single missing mode will result in reduced

0022-460X/94/410031 + 11 $08.00/0

DOFs, and thereby reduced accuracy. This problem is avoided in reference [12], where the rigid body modes are extracted from a set of measured FRFs. In terms of testing, the first method [10] requires deliberately suspending the system in a "free–free" state, the second method [11] needs accurately determined FRFs achieved by a sweep sine test, which is experimentally complicated and time-consuming, while the third method [12] uses the measured FRF from a shaker test, which takes a long time to set up. In terms of calculation, both of the first two methods use non-linear minimization methods, which require proper initial values, and take up more computation time.

In this paper a systematic method is presented to determine the rigid body characteristics using the carefully selected rigid body modes and mode shapes obtained from time domain impact data. All of the parameters are determined by solving simultaneous linear equations. If the total mass of the rigid body can be accurately measured, only the output data are needed, thus simplifying the test. Moreover, impact forces can be applied at any location in arbitrary directions to excite the rigid body modes, since the force measurement is not needed if the mass is known. The key to the success and accuracy of the method lies in the precise estimation of modal parameters by data dependent systems (DDS) methodology [13, 14].

2. FORMULATION

The system illustrated in Figure 1 is a rigid block mounted on a rigid base that is fixed, and each mount has stiffness and damping with negligible mass. Assuming viscous damping, the equation of motion with six degrees of freedom at the center of gravity (g) of the system can be expressed as

$$M_g \ddot{X}_g + C_g \dot{X}_g + K_g X_g = F_g, \tag{1}$$

where

$$M_g = \begin{bmatrix} m & 0 & 0 & 0 & 0 & 0 \\ 0 & m & 0 & 0 & 0 & 0 \\ 0 & 0 & m & 0 & 0 & 0 \\ 0 & 0 & 0 & I_{xx} & -I_{xy} & -I_{xz} \\ 0 & 0 & 0 & -I_{yx} & I_{yy} & -I_{yz} \\ 0 & 0 & 0 & -I_{zx} & -I_{zy} & I_{zz} \end{bmatrix}, \quad X_g = \begin{bmatrix} x_g \\ y_g \\ z_g \\ \theta_x \\ \theta_y \\ \theta_z \end{bmatrix}, \quad F_g = \begin{bmatrix} f_x \\ f_y \\ f_z \\ T_x \\ T_y \\ T_z \end{bmatrix}.$$

C_g and K_g are the system damping and stiffness matrices, respectively. The angular accelerations $\ddot{\theta}_x$, $\ddot{\theta}_y$, and $\ddot{\theta}_z$ are more difficult to measure than the translational accelerations. The translational accelerations $\ddot{x}_g$, $\ddot{y}_g$, and $\ddot{z}_g$ at the center of gravity are usually more difficult to measure than the motion on the surface of the rigid body. The transformation

$$X_m = T_{mg} X_g \tag{2}$$

provides the relation between the motion at the center of gravity and the p pure translational measurements on the surface, where X_m is the measurement vector with p elements,

$$X_m = [X_1, X_2, \ldots, X_p]^T.$$

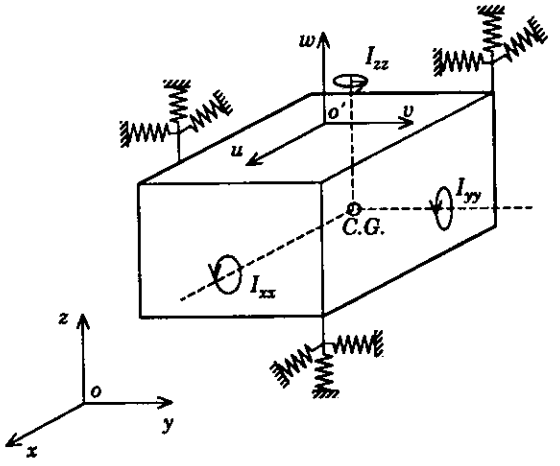

Figure 1. The rigid body and support system.

The transformation matrix T_{mg} can be formed in the following way. For any measurement $X_i\,(i = 1, 2, \ldots, p)$, it follows from the kinematics of the rigid body that the corresponding ith row of T_{mg} will be

$$\left\{\begin{array}{cccccc} [1 & 0 & 0 & 0 & w_i - w_g & v_g - v_i] \\ [0 & 1 & 0 & w_g - w_i & 0 & u_i - u_g] \\ [0 & 0 & 1 & v_i - v_g & u_g - u_i & 0] \\ [-1 & 0 & 0 & 0 & w_g - w_i & v_i - v_g] \\ [0 & -1 & 0 & w_i - w_g & 0 & u_g - u_i] \\ [0 & 0 & -1 & v_i - v_g & u_g - u_i & 0] \end{array}\right\}, \quad \text{if } X_i \text{ is in direction} \left\{\begin{array}{c} u \\ v \\ w \\ -u \\ -v \\ -w \end{array}\right\}, \tag{3}$$

where (u_i, v_i, w_i) is the co-ordinate of the location at which the ith accelerometer is mounted. If the number of measurements $p = 6$, and the p measurements X_i are properly chosen such that the rank of the matrix T_{mg} is 6, we have

$$X_g = T_{mg}^{-1} X_m. \tag{4}$$

The relation between F_g and an excitation force $F = (f_x \quad f_y \quad f_z)^{\mathrm{T}}$ at point (u_f, v_f, w_f) is

$$F_g = T_f F, \tag{5}$$

where

$$T_f = \begin{bmatrix} 1 & 0 & 0 \\ 0 & 1 & 0 \\ 0 & 0 & 1 \\ 0 & w_g - w_f & v_f - v_g \\ w_f - w_g & 0 & u_g - u_f \\ v_g - v_f & u_f - u_g & 0 \end{bmatrix}.$$

Substituting equations (4) and (5) into equation (1), and multiplying by $(T_{mg}^{-1})^{\mathrm{T}}$ on both sides, we obtain

$$M_m \ddot{X}_m + C_m \dot{X}_m + K_m X_m = F_m, \tag{6}$$

where

$$M_m = (T_{mg}^{-1})^T M_g T_{mg}^{-1}, \qquad C_m = (T_{mg}^{-1})^T C_g T_{mg}^{-1}, \qquad K_m = (T_{mg}^{-1})^T K_g T_{mg}^{-1},$$
$$F_m = (T_{mg}^{-1})^T T_f F. \tag{7–10}$$

Equation (6) is the equation of motion in terms of the measurement X_m and the input force F_m. This equation makes it possible to identify the system parameters using the measurements of translational motion (avoiding the measurements of rotation). It is easy to prove that

$$T_{mg} = T_{md} G_{dg}, \tag{11}$$

where T_{md} is of the same form as T_{mg} but with the co-ordinate $g(u_g, v_g, w_g)$ replaced by the $d(u_d, v_d, w_d)$. Furthermore,

$$G_{dg} = \begin{bmatrix} I & H_{dg} \\ 0 & I \end{bmatrix}, \tag{12}$$

$$H_{dg} = -H_{gd} = \begin{bmatrix} 0 & w_d - w_g & v_g - v_d \\ w_g - w_d & 0 & u_d - u_g \\ v_d - v_g & u_g - u_d & 0 \end{bmatrix}. \tag{13}$$

Note that matrix G_{dg} has a special property, its inverse

$$G_{dg}^{-1} = \begin{bmatrix} I & -H_{dg} \\ 0 & I \end{bmatrix} = \begin{bmatrix} I & H_{gd} \\ 0 & I \end{bmatrix} = G_{gd}, \tag{14}$$

which will be used later. Since equations (11)–(13) hold for any point $d(u_d, v_d, w_d)$, the origin $o(0, 0, 0)$ will be used for convenience.

From equations (7), (9) and (11), we obtain

$$M_m^{-1} K_m = T_{mg} M_g^{-1} K_g T_{mg}^{-1} = T_{mo} G_{og} M_g^{-1} K_g G_{og}^{-1} T_{mo}^{-1}, \tag{15}$$

i.e.,

$$M_g G_{og}^{-1} (T_{mo}^{-1} M_m^{-1} K_m T_{mo}) = K_g G_{og}^{-1}. \tag{16}$$

Since

$$G_{og}^{-1} = G_{go},$$

letting

$$Q = T_{mo}^{-1} M_m^{-1} K_m T_{mo}, \tag{17}$$

we obtain

$$M_g G_{go} Q = K_g G_{go}. \tag{18}$$

In equation (17), T_{mo} is determined by the geometric co-ordinates of the measurement point, while $M_m^{-1} K_m$ is a block of the state transition matrix [13, 15]

$$\begin{bmatrix} -M_m^{-1} C_m & -M_m^{-1} K_m \\ I & O \end{bmatrix} = \begin{bmatrix} L\mu \\ L \end{bmatrix} \mu \begin{bmatrix} L\mu \\ L \end{bmatrix}^{-1}, \tag{19}$$

where μ is the 12×12 diagonal mode matrix, the diagonal elements of which are the eigenvalues which provide frequencies of modes: the complex eigenvalues are in complex conjugate pairs. L is the corresponding 6×12 mode shape matrix, the columns of which

are the mode shapes including real and complex mode shapes: the complex mode shapes are also in complex conjugate pairs. Arranging the L and μ in block form gives

$$L = [L_1 \quad L_2], \qquad \mu = \begin{bmatrix} \mu_1 & O \\ O & \mu_2 \end{bmatrix}, \tag{20, 21}$$

where L_1, L_2, μ_1 and μ_2 are 6×6 matrices, O is a 6×6 zero matrix, and using the inverses of the partitioned matrices, equation (19) can be simplified as follows:

$$\begin{bmatrix} -M_m^{-1}C_m & -M_m^{-1}K_m \\ I & O \end{bmatrix} = \begin{bmatrix} L_1\mu_1 L_1^{-1} + L_2\mu_2 L_2^{-1} & -(L_1\mu_1 L_1^{-1})(L_2\mu_2 L_2^{-1}) \\ I & O \end{bmatrix}, \tag{22}$$

so that

$$M_m^{-1}C_m = -(L_1\mu_1 L_1^{-1} + L_2\mu_2 L_2^{-1}), \qquad M_m^{-1}K_m = (L_1\mu_1 L_1^{-1})(L_2\mu_2 L_2^{-1}). \tag{23, 24}$$

The importance of equation (22) is that it reduces the inverse of a 12×12 complex matrix to the inverse of two 6×6 complex matrices. It also provides the simple and compact formulas to calculate $M_m^{-1}C_m$ and $M_m^{-1}K_m$. If there is no real mode, the complex modes and mode shapes can be arranged in a way such that L_2 and μ_2 are the complex conjugates of L_1 and μ_1. Then, equations (23) and (24) become

$$M_m^{-1}C_m = -(L_1\mu_1 L_1^{-1} + \overline{L_1\mu_1 L_1^{-1}}) = -2\,\mathrm{Re}\,(L_1\mu_1 L_1^{-1}), \tag{25}$$

$$M_m^{-1}K_m = (L_1\mu_1 L_1^{-1})(\overline{L_1\mu_1 L_1^{-1}}) = \mathrm{Re}^2\,(L_1\mu_1 L_1^{-1}) + \mathrm{Im}^2\,(L_1\mu_1 L_1^{-1}). \tag{26}$$

The notation $\mathrm{Re}\,(A)$ represents the real part of the complex matrix A, and $\mathrm{Im}\,(A)$ represents the imaginary part of A.

In addition, if complex modes are proportionally damped, the mode shapes are real, and we obtain

$$M_m^{-1}C_m = -2L_1\,\mathrm{Re}\,(\mu_1)L_1^{-1}, \qquad M_m^{-1}K_m = L_1[\mathrm{Re}^2\,(\mu_1) + \mathrm{Im}^2\,(\mu_1)]L_1^{-1}. \tag{27, 28}$$

Substituting equation (24) into equation (17), we have

$$Q = T_{mo}^{-1}(L_1\mu_1 L_1^{-1})(L_2\mu_2 L_2^{-1})T_{mo}. \tag{29}$$

Equation (29) shows that Q is known once the modes, mode shapes and the geometric locations of the measurement are known. When the number of measurements $p > 6$, equation (29) can be easily extended, using the generalized inverse, to

$$Q = T_{mo}^{\dagger}(L_1\mu_1 L_1^{\dagger})(L_2\mu_2 L_2^{\dagger})T_{mo}, \tag{30}$$

where the generalized inverse of an $m \times n$ $(m > n)$ matrix A is defined as

$$A^{\dagger} = (A^{\mathrm{T}}A)^{-1}A^{\mathrm{T}},$$

assuming that $(A^{\mathrm{T}}A)^{-1}$ exists. Substituting into equation (18)

$$M_g = \begin{bmatrix} mI & 0 \\ 0 & M_2 \end{bmatrix}, \quad K_g = \begin{bmatrix} K_{11} & K_{12} \\ K_{21} & K_{22} \end{bmatrix}, \quad G_{go} = \begin{bmatrix} I & H_{go} \\ 0 & I \end{bmatrix}, \quad Q = \begin{bmatrix} Q_{11} & Q_{12} \\ Q_{21} & Q_{22} \end{bmatrix},$$

we obtain

$$\begin{bmatrix} m(Q_{11} + H_{go}Q_{21}) & m(Q_{12} + H_{go}Q_{22}) \\ M_2Q_{21} & M_2Q_{22} \end{bmatrix} = \begin{bmatrix} K_{11} & K_{11}H_{go} + K_{12} \\ K_{21} & K_{21}H_{go} + K_{22} \end{bmatrix}, \tag{31}$$

which provides the following four matrix equations

$$m(Q_{11} + H_{go}Q_{21}) = K_{11}, \qquad m(Q_{12} + H_{go}Q_{22}) = K_{11}H_{go} + K_{12}, \tag{32, 33}$$

$$M_2Q_{21} = K_{21}, \qquad M_2Q_{22} = K_{21}H_{go} + K_{22}. \tag{34, 35}$$

Because K_{11} is symmetric, the right side of equation (33) has to be symmetric: therefore, the center of gravity $g(u_g, v_g, w_g)$ and the elements of matrix Q satisfy

$$\begin{bmatrix} q_{52} + q_{63} & -q_{42} & -q_{43} \\ -q_{51} & q_{41} + q_{63} & -q_{53} \\ -q_{61} & -q_{62} & q_{41} + q_{52} \end{bmatrix} \begin{bmatrix} u_g \\ v_g \\ w_g \end{bmatrix} = \begin{bmatrix} q_{32} - q_{23} \\ q_{13} - q_{31} \\ q_{21} - q_{12} \end{bmatrix}, \tag{36}$$

which gives the center of gravity u_g, v_g and w_g. Once the center of gravity is determined, K_{11}, K_{12} and K_{22} can be determined from equations (32)–(35), as ratios to mass m:

$$K_{11}/m = (Q_{11} + H_{go}Q_{21}), \qquad K_{12}/m = Q_{12} + H_{go}Q_{22} - Q_{11}H_{go} - H_{go}Q_{21}H_{go}, \tag{37, 38}$$

and since $K_{21} = K_{12}^{\mathrm{T}}$,

$$M_2/m = (K_{12}^{\mathrm{T}}/m)Q_{21}^{-1}, \qquad K_{22}/m = (K_{12}^{\mathrm{T}}/m)Q_{21}^{-1}Q_{22} - Q_{21}H_{go}. \tag{39, 40}$$

The above derivation shows that, with the known $M_m^{-1}K_m$, we could determine the center of gravity, and the ratios K_{11}/m, K_{12}/m, K_{21}/m, K_{22}/m and M_2/m, as shown in equations (36)–(40). Once m is known, the stiffness matrix K_g and the moment of inertia matrix M_2 can be determined.

3. EXPERIMENTAL RESULTS

This method has been tested using computer simulation data [15]; it shows that accurate result can be achieved using accurate data. Here we show that reasonable result can also be obtained using experimental data. The tested system is shown in Figure 2. A rigid block is supported by three helical springs. The block is composed of two parts. The bottom part is a circular plate with a concentric hole, its dimensions being $R = 9{\cdot}25$ in, $r = 3{\cdot}5$ in and $h = 1{\cdot}5$ in. The top part is a rectangular plate, with dimensions $a = 15$ in, $b = 9$ in and $c = 1$ in. The top part and the bottom part are rigidly connected. The distance from the top surface of the top part to the bottom surface of the bottom part is 2.5 in. The two parts have a total weight of 136 lb.

The following procedure is recommended and followed for the test.

(1) Set up the data collection equipment.

(2) Select a co-ordinate system so that the accelerometers can be mounted along the corresponding x-, y- and z-axes.

(3) Determine the locations and directions for mounting the sensors. This step is very important and the following rules must be followed: (i) there must be at least one sensor for each direction x, y and z; (ii) the total number of sensors for all three directions cannot

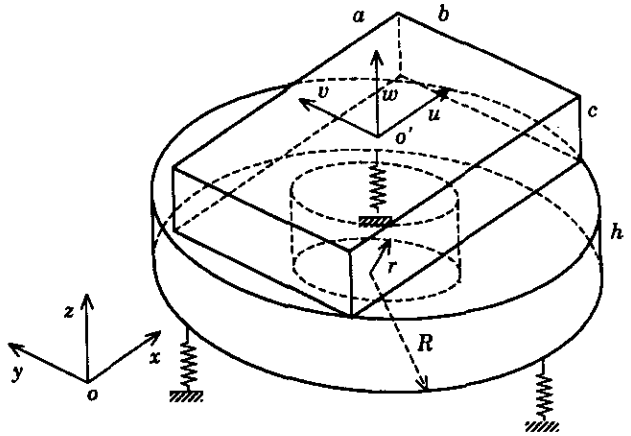

Figure 2. The rigid body test set-up: $m = 136$ lb, $R = 9{\cdot}25$ in, $r = 3{\cdot}5$ in, $h = 1{\cdot}5$ in, $a = 15$ in, $b = 9$ in, $c = 1$ in.

be less than six; the rank of the resulting transformation matrix T_{mo} must be 6—in other words, T_{mo} must have a generalized inverse.

(4) Mount the sensors at the determined locations. Make sure that the sensors for one direction are indeed parallel to each other and that the sensors for different directions are perpendicular to each other.

(5) Excite the rigid body with an impact hammer and collect acceleration data.

Following the above procedure, the center of the top surface of the rectangular plate is chosen as the origin $o'(0, 0, 0)$ of the co-ordinate system. Six accelerometers are mounted at six different points, the co-ordinates and directions of which are shown in Table 1. Therefore,

$$T_{mo} = \begin{bmatrix} 0 & 0 & 1 & v_1 & -v_1 & 0 \\ 1 & 0 & 0 & 0 & w_2 & -v_2 \\ 0 & -1 & 0 & w_3 & 0 & -u_3 \\ 0 & 1 & 0 & -w_4 & 0 & u_4 \\ 0 & 0 & 1 & v_5 & -u_5 & 0 \\ 0 & 0 & -1 & -v_6 & u_6 & 0 \end{bmatrix} = \begin{bmatrix} 0 & 0 & 1 & 1{\cdot}5 & -6{\cdot}75 & 0 \\ 1 & 0 & 0 & 0 & -0{\cdot}8 & -5{\cdot}7 \\ 0 & -1 & 0 & 0{\cdot}75 & 0 & -7{\cdot}25 \\ 0 & 1 & 0 & 3{\cdot}25 & 0 & -8{\cdot}4 \\ 0 & 0 & 1 & -4{\cdot}0 & -4{\cdot}5 & 0 \\ 0 & 0 & -1 & 0{\cdot}7 & -9{\cdot}0 & 0 \end{bmatrix}.$$

The test system is excited using an impact hammer, and the time domain data of the six measurement points are collected simultaneously using an HP3566A/HP3567A eight-channel network analyzer. The modes and mode shapes, obtained using DDS methodology from the measurement data [13], are listed in Table 2. Since the complex parts of the mode

TABLE 1

The co-ordinates and directions of the measurement points

Number	u	v	w	Direction
1	6·75	1·5	0·0	z
2	2·0	5·7	−0·8	x
3	7·25	2·0	0·75	$-y$
4	−8·4	−0·75	−3·25	y
5	4·5	−4·0	0·0	z
6	−9	−0·7	−2·5	$-z$

shapes are all so small, we can use equations (25) and (26) instead of equations (23) and (24). Substituting these modes and mode shapes and T_{mo} into equation (26), we obtain

$$Q = \begin{bmatrix} 1613{\cdot}11 & -37{\cdot}83 & 67{\cdot}11 & -647{\cdot}75 & -1117{\cdot}11 & -696{\cdot}94 \\ 106{\cdot}00 & 1564{\cdot}25 & 44{\cdot}29 & -749{\cdot}26 & -1049{\cdot}95 & 1236{\cdot}32 \\ 143{\cdot}16 & 40{\cdot}18 & 1649{\cdot}67 & -72{\cdot}15 & -989{\cdot}41 & 1086{\cdot}43 \\ -40{\cdot}03 & 152{\cdot}31 & -25{\cdot}30 & 3978{\cdot}81 & -131{\cdot}29 & -402{\cdot}64 \\ -118{\cdot}28 & -49{\cdot}02 & -19{\cdot}61 & -213{\cdot}94 & 2759{\cdot}45 & -20{\cdot}42 \\ -8{\cdot}51 & 14{\cdot}83 & 26{\cdot}25 & -156{\cdot}01 & 19{\cdot}72 & 3382{\cdot}46 \end{bmatrix}.$$

Solution of equation (36) gives

$$\begin{bmatrix} u_g \\ v_g \\ w_g \end{bmatrix} = \begin{bmatrix} -0{\cdot}28 \\ -0{\cdot}18 \\ -1{\cdot}57 \end{bmatrix}.$$

Hence

$$H_{go} = \begin{bmatrix} 0 & w_g & -v_g \\ -w_g & 0 & u_g \\ v_g & -u_g & 0 \end{bmatrix} = \begin{bmatrix} 0 & -1{\cdot}57 & 0{\cdot}17 \\ 1{\cdot}57 & 0 & -0{\cdot}26 \\ -0{\cdot}17 & 0{\cdot}26 & 0 \end{bmatrix}.$$

Substituting H_{go} into equations (37)–(40), we obtain

$$\frac{K_{11}}{m} = \begin{bmatrix} 1803{\cdot}80 & 51{\cdot}51 & 100{\cdot}76 \\ 51{\cdot}51 & 1806{\cdot}62 & -4{\cdot}38 \\ 100{\cdot}76 & -4{\cdot}38 & 1647{\cdot}45 \end{bmatrix} \quad (1/s^2),$$

$$\frac{K_{12}}{m} = \begin{bmatrix} -373{\cdot}43 & -2590{\cdot}61 & -34{\cdot}41 \\ 2708{\cdot}34 & -1166{\cdot}29 & 194{\cdot}55 \\ -447{\cdot}49 & -379{\cdot}88 & 1141{\cdot}42 \end{bmatrix} \quad (\text{in}/s^2) = \frac{K_{21}^{\mathrm{T}}}{m},$$

$$\frac{K_{22}}{m} = \begin{bmatrix} 70\,117{\cdot}25 & -11\,857{\cdot}46 & -13\,628{\cdot}94 \\ -12\,883{\cdot}41 & 59\,331{\cdot}80 & 3188{\cdot}55 \\ -16\,919{\cdot}95 & 3273{\cdot}89 & 141417{\cdot}10 \end{bmatrix} \quad (\text{in}^2/s^2),$$

$$\frac{M_2}{m} = \begin{bmatrix} 16{\cdot}93 & -2{\cdot}33 & -2{\cdot}05 \\ -0{\cdot}62 & 21{\cdot}35 & 0{\cdot}72 \\ -2{\cdot}53 & 0{\cdot}74 & 41{\cdot}53 \end{bmatrix} \quad (\text{in}^2).$$

To obtain a symmetric M_2, the average values

$$\tfrac{1}{2}\left(\frac{M_2}{m} + \frac{M_2^{\mathrm{T}}}{m}\right) = \begin{bmatrix} 16{\cdot}93 & -1{\cdot}48 & -2{\cdot}29 \\ -1{\cdot}48 & 21{\cdot}35 & 0{\cdot}73 \\ -2.29 & 0{\cdot}73 & 41{\cdot}53 \end{bmatrix} \quad (\text{in}^2)$$

is taken as M_2/m. Therefore, we have

$$M_g = \begin{bmatrix} mI & 0 \\ 0 & M_2 \end{bmatrix} = \begin{bmatrix} 1 & 0 & 0 & 0 & 0 & 0 \\ 0 & 1 & 0 & 0 & 0 & 0 \\ 0 & 0 & 1 & 0 & 0 & 0 \\ 0 & 0 & 0 & 16{\cdot}93 & -1{\cdot}48 & -2{\cdot}29 \\ 0 & 0 & 0 & -1{\cdot}48 & 21{\cdot}35 & 0{\cdot}73 \\ 0 & 0 & 0 & -2{\cdot}29 & 0{\cdot}73 & 41{\cdot}53 \end{bmatrix} m.$$

TABLE 2

Modes and mode shapes

	First mode		Second mode		Third mode	
	Frequency	6·1009	Frequency	6·2980	Frequency	6·4216
	Damping	0·3914	Damping	0·3951	Damping	0·0453
	Real	−0·1501	Real	−0·1564	Real	−0·01829
	Imaginary	38·33264	Imaginary	39·57110	Imaginary	40·34827
	Mode shape		Mode shape		Mode shape	
Number	Real	Imaginary	Real	Imaginary	Real	Imaginary
1	−1·0821	0·0414	−0·1106	0·0589	0·4711	0·0126
2	1·0000	0·0000	−0·0826	0·0836	0·2429	−0·0053
3	0·1276	−0·0527	1·0000	−0·0000	−0·1372	−0·0031
4	0·0324	−0·0561	0·9865	0·0236	0·0465	−0·0016
5	−0·9444	0·0047	0·3203	0·0443	0·4604	0·0049
6	0·5202	0·0281	0·2894	0·2074	1·0000	−0·0000

	Fourth mode		Fifth mode		Sixth mode	
	Frequency	8·5660	Frequency	9·1984	Frequency	10·1250
	Damping	0·1112	Damping	0·1926	Damping	0·1334
	Real	−0·05986	Real	−0·11132	Real	−0·08490
	Imaginary	53·82165	Imaginary	57·79512	Imaginary	63·61917
	Mode shape		Mode shape		Mode shape	
Number	Real	Imaginary	Real	Imaginary	Real	Imaginary
1	−0·9126	−0·0044	0·3510	−0·0063	0·4640	0·0000
2	−0·2970	−0·0004	−0·7959	−0·0018	0·2816	0·0013
3	−0·0573	−0·0043	1·0000	0·0000	−0·5906	0·0007
4	−0·1209	0·0024	−0·8421	−0·0019	1·0000	0·0000
5	−0·7884	0·0042	−0·0322	−0·0074	−0·7039	0·0094
6	1·0000	−0·0000	−0·1644	0·0035	−0·3847	0·0024

Since the mass $m = 136$ lb, we obtain the moment of inertia matrix

$$M_e = \begin{bmatrix} 2303 & -201 & -311 \\ -201 & 2904 & 99 \\ -311 & 99 & 5648 \end{bmatrix}.$$

Also,

$$K_g = \begin{bmatrix} K_{11} & K_{12} \\ K_{21} & K_{22} \end{bmatrix}$$

$$= \begin{bmatrix} 1803{\cdot}80 & 51{\cdot}51 & 100{\cdot}76 & -373{\cdot}43 & -2590{\cdot}61 & -344{\cdot}06 \\ 51{\cdot}51 & 1806{\cdot}62 & -4{\cdot}38 & 2708{\cdot}34 & -1166{\cdot}29 & 194{\cdot}75 \\ 100{\cdot}76 & -4{\cdot}38 & 1647{\cdot}45 & -447{\cdot}49 & -379{\cdot}88 & 1141{\cdot}42 \\ -373{\cdot}43 & 2708{\cdot}34 & -447{\cdot}49 & 70\,117{\cdot}25 & -11\,857{\cdot}46 & -13\,628{\cdot}94 \\ -2590{\cdot}61 & -1166{\cdot}29 & -379{\cdot}88 & -12\,883{\cdot}41 & 59\,331{\cdot}80 & 3188{\cdot}55 \\ -344{\cdot}06 & 194{\cdot}75 & 1141{\cdot}42 & -16\,919{\cdot}95 & 3273{\cdot}89 & 141\,417{\cdot}10 \end{bmatrix}.$$

TABLE 3

Comparison of identified result with calculated values

Characteristics	Calculated value	Identified value	Difference (%)
u_g (in)	0	−0·26	1·4
v_g (in)	0	−0·18	1·0
w_g (in)	−1·40	−1·57	6·8
I_{xx} (lb in^2)	2652	2302	13
I_{yy} (lb in^2)	3087	2904	5·9
I_{zz} (lb in^2)	5440	5648	3·8
I_{xy} (lb in^2)	0	201	—
I_{xz} (lb in^2)	0	311	—
I_{yz} (lb in^2)	0	−99	—

A comparison of the calculated values with the values identified using vibration data and the known mass is shown in Table 3. The identified values are in very good agreement with the calculated values. The differences for the center of gravity are within 0·3 in, and their ratio over the total length in the corresponding direction is less that 7%. The differences for the moment of inertia are within 13%, while the moments of products are fairly small compared to the moment of inertia. Generally, the center of gravity and stiffness matrix are not as sensitive to measurement noise as the moment of inertia. The moments of inertia are more sensitive to measurement noise, but the result is still quite reasonable. These errors may be contributed by (i) co-ordinate measurement error, (ii) the directions of the sensors not being as parallel or perpendicular as desired, or (iii) the measurement signal for certain modes being much stronger than for certain other modes, which results in a small modal signal to noise ratio. Note that the calculated values of the center of gravity and moment of inertia are themselves subject to measurement errror of geometric dimensions.

In Table 4 the above result is compared with those of DSIM [9] and of Conti and Bretl [12]. Because the true values for those results are unknown, they are compared with the results tested by the traditional (pendulum) method.

4. CONCLUSIONS

A new identification method has been developed, which determines the center of gravity, the moments of inertia, and the damping and stiffness matrices of the rigid body system. Only output vibration data are used, based on a simple hammer test. The test result proved that reasonably good results can be achieved using such a simple and rapid test method. All of the identified parameters are obtained through matrix transformations and solutions

TABLE 4

Comparison of accuracy with published methods (Errors)

Characteristics	DSIM [9]	Conti and Bretl [12]	Proposed method
u_g (in)	0·23	0·83	0·26
v_g (in)	0·35	0·55	0·18
w_g (in)	0·92	0·24	0·17
I_{xx} (%)	9·2	0·5	13
I_{yy} (%)	1·2	3·0	5·9
I_{zz} (%)	7·8	18·0	3·8

of simultaneous linear equations, which makes the method computationally fast and easy to implement.

REFERENCES

1. T. SEINO, M. FURUSAWA and H. IKUMA 1983 *SAE paper* 830088. On the theory of orthogonal engine mount system and its application to motorcycles.
2. A. MATSUDA, Y. HAYASHI and J. HASEGAWA 1987 *SAE paper* 870964. Vibration analysis of a diesel engine at cranking and idling modes and its mounting system.
3. C. J. RADCLIFFE, M. N. PICKLEMANN, C. E. SPIEKERMANN and D. S. HINE 1983 *SAE paper* 830259. Simulation of engine idel shake vibration.
4. D. M. FORD 1985 *SAE paper* 850976. An analysis and application of a decoupled engine mount system for idle isolation.
5. J. E. BERNARD and J. M. STARKEY 1983 *SAE paper* 830257. Engine mount optimization.
6. P. E. GECK and P. E. PATTON 1984 *SAE paper* 840736. Front wheel drive engine mount optimization.
7. H. HATA and H. TANAKA 1987 *SAE paper* 870961. Experimental method to derive optimum engine mount system for idle shake.
8. N. OKUBO and T. FURUKAWA 1984 *Proceedings of the 2nd IMAC*, 544–549. Measurement of rigid body modes for dynamic design.
9. T. BUTSUEN, M. OKUMA and A. NAGAMATSU 1986 *SAE paper* 860551. Application of direct system identification method for engine rigid body mount system.
10. M. OKUMA and A. NAGAMATSU 1987 *Japan Society of Mechanical Engineers, International Journal* **30**, 970–975. Experimental identification of a mechanical structure with characteristic matrices (proposed method with input data in which noise is included).
11. M. OKUMA, T. OHARA, K. NAGAO and A. NAGAMATSU 1989 *SAE paper* 891139. Application of a new experimental identification method to engine rigid body mount system.
12. P. CONTI and J. BRETL 1989 *Transactions of the American Society of Mechanical Engineers, Journal of Vibration, Acoustics, Stress, and Reliability in Design* **111**, 134–138. Mount stiffnesses and inertia properties from modal test data.
13. S. M. PANDIT 1991 *Modal and Spectrum Analysis: Data Dependent Systems in State Space*. New York: Wiley Interscience.
14. S. M. PANDIT and N. P. MEHTA 1985 *Transactions of the American Society of Mechanical Engineers, Journal of Dynamic Systems Measurement and Control* **107**, 132–138. Data dependent systems approach to modal analysis via state space.
15. Z. Q. HU 1991 *Ph.D. dissertation, Michigan Technological University*. Identification of rigid body characteristics and support properties through modal analysis.